

---

This item was submitted to [Loughborough's Research Repository](#) by the author.  
Items in Figshare are protected by copyright, with all rights reserved, unless otherwise indicated.

## Quasi-constant volume (QCV) spark ignition combustion

PLEASE CITE THE PUBLISHED VERSION

<http://www.sae.org/congress/2009/>

PUBLISHER

© SAE International

VERSION

VoR (Version of Record)

LICENCE

CC BY-NC-ND 4.0

REPOSITORY RECORD

Chen, Rui, Edward Winward, Paul Stewart, Ben Taylor, and Dan Gladwin. 2011. "Quasi-constant Volume (QCV) Spark Ignition Combustion". figshare. <https://hdl.handle.net/2134/8413>.

This item was submitted to Loughborough's Institutional Repository (<https://dspace.lboro.ac.uk/>) by the author and is made available under the following Creative Commons Licence conditions.



For the full text of this licence, please go to:  
<http://creativecommons.org/licenses/by-nc-nd/2.5/>

2009-01-0700

## Quasi-Constant Volume (QCV) Spark Ignition Combustion

Rui Chen and Edward Winward  
Loughborough University, UK

Paul Stewart  
University of Salford, UK

Ben Taylor and Dan Gladwin  
Sheffield University, UK

Copyright © 2009 SAE International

### ABSTRACT

The Otto cycle delivers theoretical maximum thermal efficiency. The traditional design of internal combustion engines using a simple slide-crank mechanism gives no time for a constant volume combustion which significantly reduces the cycle efficiency. In this study, using a high torque, high bandwidth, permanent magnet electric drive system attached to the crankshaft, variable angular velocities of the engine crankshaft were implemented. The system enabled reductions in piston velocity around the top dead centre region to a fraction of its value at constant crankshaft angular velocity typical in conventional engines. A quasi-constant volume combustion has thus been successfully achieved, leading to improvements in engine fuel consumption and power output which are discussed in detail.

### INTRODUCTION

There is an urgent need for a new generation of automobile power plants with improved fuel efficiency and reduced pollutant emissions to satisfy demands worldwide for both energy conservation and environmental protection. Conventional Internal Combustion (IC) engines are based on a crank-rod-slider mechanism, which provides a relatively simple solution to achieve a thermodynamic cycle while providing mechanical power. While the performance, emissions and reliability of IC engines have been

improved significantly, the fundamental principle remains largely unaltered. Indeed, modern IC engines operate on a mechanical cycle rather than a thermodynamic cycle [1]. In theory, the most efficient thermodynamic cycle for IC engines is the Otto cycle [2], which consists of isentropic compression and expansion processes and constant volume heat addition and rejection processes. Arguably, the most important parts of the cycle, which determine the efficiency, are the constant volume heat addition at high compression ratios, since this provides the highest thermal potential of the various possible thermodynamic cycles which are suitable for IC engines, and the subsequent expansion process, which converts the thermal potential into work. In reality, neither conventional Spark Ignition (SI) nor Compression Ignition (CI), or even the newly developed Homogeneous Charge Compression Ignition (HCCI) or Controlled Auto Ignition (CAI) combustion processes, can achieve the efficiency level suggested by the ideal thermodynamic cycles [3]. The main difficulties are due to the geometric cycle of the piston movement and the requirement that the engine delivers smooth rotation to the mechanical clutch and vehicle transmission.

During operation of conventional IC engines, the piston can only reciprocate continuously between Top Dead Centre (TDC) and Bottom Dead Centre (BDC) at a frequency proportional to the engine speed. The chemical reaction process associated with combustion events, however, essentially takes a fixed-time to

The Engineering Meetings Board has approved this paper for publication. It has successfully completed SAE's peer review process under the supervision of the session organizer. This process requires a minimum of three (3) reviews by industry experts.

All rights reserved. No part of this publication may be reproduced, stored in a retrieval system, or transmitted, in any form or by any means, electronic, mechanical, photocopying, recording, or otherwise, without the prior written permission of SAE.

ISSN 0148-7191

Positions and opinions advanced in this paper are those of the author(s) and not necessarily those of SAE. The author is solely responsible for the content of the paper.

**SAE Customer Service:** Tel: 877-606-7323 (inside USA and Canada)  
Tel: 724-776-4970 (outside USA)  
Fax: 724-776-0790  
Email: [CustomerService@sae.org](mailto:CustomerService@sae.org)

**SAE Web Address:** <http://www.sae.org>

Printed in USA



**SAE**International

complete, which is relatively independent of the engine speed. In order to maximize the work obtained from the heat energy released by combustion, the air/fuel mixture has to be ignited prior to the piston reaching TDC, and the ignition timing should be adjusted according to the engine speed and the quality of the air/fuel mixture. Clearly, the early stage of the heat release before the piston reaches TDC results in negative work. During the combustion event, the piston movement is defined by the crank rotation, so that truly constant volume heat release is not achievable. Further, to efficiently scavenge the burned gas, the exhaust valve has to be opened well before BDC, while the pressure of the burned gas is still high. Thus, a large portion of the thermal energy is expelled into the exhaust, which further reduces the engine efficiency.

The ideal scenario is to initiate and complete the combustion event while the piston remains at the TDC position. This provides the maximum thermal potential and eliminate the negative work due to early ignition which is well into compression stroke with conventional engine strategies. In addition, if the combustion event completes at the TDC, the effective expansion stroke can be maximally extended to fully use the thermal energy as well as to provide sufficient time for post-combustion reactions, thereby reducing partial burned emissions. One practical method of achieving such an optimization without changing the engine design and sacrificing engine performances is to significantly reduce the engine crank rotation velocity at the TDC position to provide extra time for completing the combustion. The engine is accelerated during compression and expansion phases to maintain the high average crank speed to deliver the high power output. This will then generate a new combustion cycle which sit between conventional IC engine combustion cycle and ideal Otto constant volume combustion cycle. This can therefore be named as a Quasi-Constant Volume (QCV) combustion cycle, as illustrated in Figure 1.

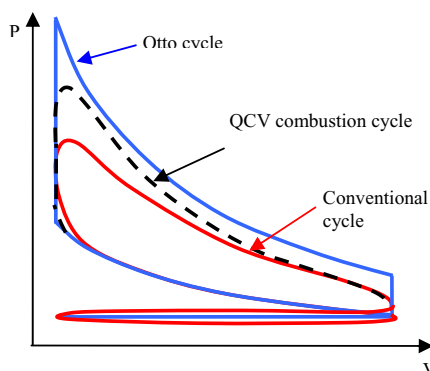


Figure 1: Typical P-V diagram

Theoretically, series-hybrid power-train enables a higher efficiency from IC engine configurations [4]. The QCV

concept offers a potential for higher combustion efficiency. It can be combined with a sophisticated combined electric motor and generator unit to form a series-hybrid powertrain to deliver the much desired high fuel efficiency and low pollutant emissions powertrain system with good power output.

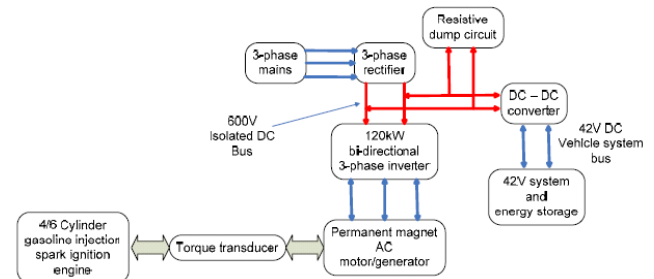


Figure 2: Schematic QCV combustion system

## PROOF-OF-PRINCIPLE

In order to facilitate the QCV combustion concept, a proof-of-principle engine system has been developed as shown in Figure 2. The systems consists of a high torque-to-inertia, high bandwidth, permanent magnet brushless AC (PMA) electric machine, a single-cylinder research Spark Ignition (SI) engine, and a control system.



Figure 3: The QCV engine

ENGINE - The engine employed in this research, as shown in Figure 3, is a single cylinder research engine. Its combustion chamber, the head and the piston, is based on the GM Family One 1.8 litre engine architecture, 4-valve with a bore of 80.5mm and a stroke of 88.2mm. The bottom part of the engine is converted from a twin-cylinder engine block. The combustion chamber has been lifted significantly from the bottom.

The extension in between is reserved for further future work. The piston is connected to a conventional connecting rod designed for the original twin-cylinder engine block by a stiff steel bar sliding with the piston. This adds a significant extra mass to the small end of the connecting rod. The piston in the second cylinder has been left open and the piston is redesigned to balance the extra mass.

**MOTOR/GENERATOR** - The engine was attached directly at the end of the crankshaft to a 200Nm, low inertia, permanent magnet brushless AC servo-motor. The servo motor is connected to a high-bandwidth, 3-phase, fully regenerative, AC drive rated at 100kW.

which, in turn was driven by an electric machine acts as a generator during the IC engine combustion stroke and as a control motor when necessary during the inlet, exhaust and compression strokes. The input/output power of the motor/generator controls the crankshaft trajectory at all times, so that various crankshaft angular

rotation velocities can be realized and the electrical power generation to be achieved.

The electric machine acts as a generator during the IC engine power stroke and as a control motor when necessary during the inlet, exhaust and compression strokes. The input/output power of the motor/generator controls the crankshaft trajectory at all times, so that various crankshaft angular rotation velocities can be realized and the electrical power generation to be achieved.

The demanding dynamic trajectory control and the highly transient electrical power flows are too arduous for commercially available electrical machines/drives. Therefore, the Electrical Machines and Drives Group, which has an outstanding track record for realizing innovative solutions for similarly challenging and high performance applications, will realize a custom designed water-cooled, high-bandwidth, low inertia machine/drive to perform at the level which is required to fully explore

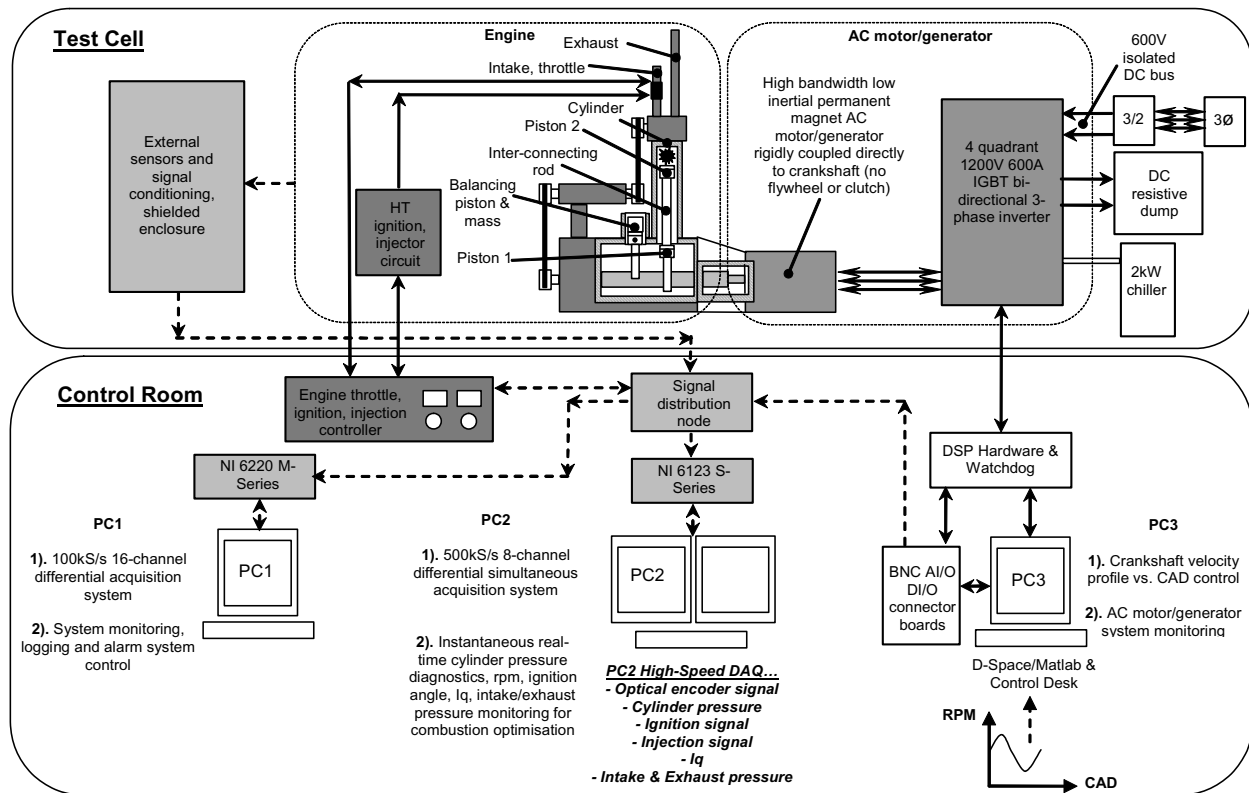


Figure 4 The QCV system and test rig

the PV envelope of the Otto cycle, with a thermal performance to cope with the arduous duty cycle. The engine mapping for injection, spark and throttle for the proposed operating regime is, as yet, unknown, as is the wide array of potential piston trajectories, including some based on polynomial design, which will be evaluated to minimize accelerations, and, hence, vibration in the engine.

**CONTROL** - Real-time engine management and electrical machine control was via a DSpace hardware development platform, and experiments were conducted to investigate the possibility of attaining a true Otto cycle.

In particular, Direct Torque Control (DTC) [5] which directly controls the flux and the electromagnetic torque by establishing a relationship between torque, flux and optimal inverter switching will be implemented. In terms of dynamic performance, DTC is expected to deliver a torque response more than 10 times faster [6] than conventional vector control methods. In addition, DTC controlled drives exhibit significantly less low-frequency torque-ripple than Pulse Width Modulation (PWM) controlled drives [7,8]. Final optimization and analysis with respect to power and combustion will take place in this phase via the application of constrained hardware-in-the-loop optimization techniques [9,10].

**TEST RIG** - To date, the experiments have been limited by the thermal and dynamic rating of the off-the-shelf commercial electrical machine. Nonetheless, it has been possible to achieve quasi-constant volume combustion by actively braking the crankshaft as the piston passed through TDC to a much lower velocity.

Figure 4 illustrates the test rig of the study. The rig consists of engine, AC motor generator, and control systems. For combustion control, a hardware based system was chosen rather than software to ensure reliability and this was designed and manufactured at Loughborough University. This system integrates the controls for ignition, fuel injection and throttle angle into a single unit called the SWIFT controller – Synchronized Wide-range Ignition Fuel Throttle controller.

A conventional ECU based system was avoided due to the need for high crankshaft angular resolution combined with the capability to maintain precise timing with high angular deceleration/acceleration within a narrow crank angle (CA) window.

The SWIFT controller uses Programmable Integrated Circuits (PIC) and was designed to be quickly reconfigured to work with a completely free piston engine design; where there exists no crankshaft position based ignition/fuel timing control. SWIFT by default operates open loop with fuelling manually controlled

based on lambda, a closed loop function is also available.

An optical encoder with a resolution 0.5 deg CA was rigidly mounted to the engine crankshaft to provide continuous crankshaft position and an optical pick-up monitored a sprocket on the belt drive to the camshafts to register the camshaft phase. These were used as inputs to SWIFT as the basis for the timing control. The ignition, fuel and throttle systems can all be isolated to validate individual system function and there is an integrated system emergency stop for engine and electric motor system shutdown.

For ignition timing control, an Excel macro has been specially written to calculate the CA position at which the ignition coil should begin to charge, this is based upon the ignition angle desired, the coil dwell period and the crankshaft angular velocity profile. SWIFT can be programmed with a coil-dwell period of 2-5 ms with a 0.1 ms resolution and has a pre-set range of coil charge angles from 60 degrees BTDC and 20 degrees ATDC and this can be easily extended by reprogramming the PIC's. In this way, the ignition angle can be controlled to within 0.5 deg CA regardless of the crankshaft angular velocity profile.

Initial fuel injection duration is determined through bilinear interpolation of an adjusted engine fuel map provided by Lotus Engineering. The interpolation is performed in an Excel look-up table and the duration (ms) is then entered into SWIFT. SWIFT has the capability to produce a single injection pulse width with a range of 1–8 ms and a resolution of .01ms. Fuel is injected as a single pulse into the intake manifold at TDC. Depending upon throttle angle, a rich mixture is required for engine start and is then adjusted to achieve lambda 1. SWIFT can be quickly adapted to provide two pulses per cycle if required.

The throttle is actuated using stepper motor controlled by SWIFT with a precision feedback of throttle angle. The rate at which the throttle is opened/closed can be changed via SWIFT and the throttle angle set to a precision of less than 1% of the WOT angle.

Labview based software monitors the engine and electric motor using thermocouple, pressure, air-flow and lambda sensors with a sample rate of 10Hz. A NI 6220 M-Series PCI card is used to process the signals. An intelligent alarm system provides synthesized voice alarms to optimize the intervention measures.

Real-time in-cylinder pressure diagnostics and electric motor/generator current/torque/power monitoring is provided by a NI 6123 S-Series 8 channel simultaneous PCI card. This system displays the 0.5 deg CA resolved crankshaft speed, ignition angle, fuel injection timing, cylinder pressure, IMEP, p-v diagram, heat release,

intake manifold pressure and electric motor current; all data is referenced to crank angle position and combustion stroke. This real-time combustion diagnostics is critical and is used to optimize the whole of the hybrid powertrain.

Rather than record data at the base crankshaft encoder resolution of 0.5 deg CA, a technique is used whereby the data are recorded at a sample rate between 100-500 KHz. This is done because it maintains a constant time base, regardless of the crankshaft angular velocity profile. Thus, when the angular velocity (and hence base encoder frequency) is reduced about TDC, a high sample rate is maintained to capture the full details of the combustion event. The single cylinder engine used in the project is for proof-of-principle. It has no cooling system. The time available for each test, especially with fired cycles, is limited before being over heated. Typical log duration is about 5 seconds and sufficient for slightly more than 30 consecutive cycles. The data are recorded to a binary file format.

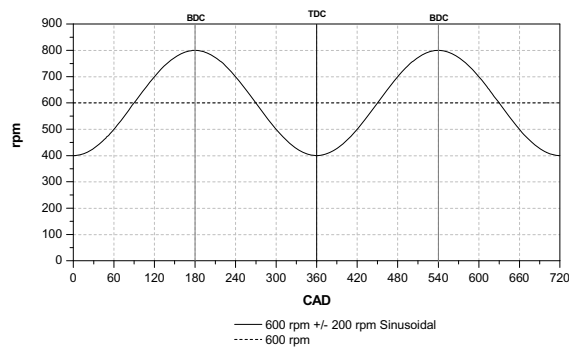


Figure 5: Conventional constant and variable sinusoidal crank velocity

The binary data files are converted to text files and processed by a specially configured Matlab M-Script. This uses the recorded crankshaft encoder TDC and CA delimiter marker (CDM) signals to determine the 0.5 deg CA intervals in the data. Interpolation is used between each 0.5 deg transition to assign a crank angle position to each sample point. The data can thus be analyzed in both time and crank angle domains at high resolution.

**PISTON TRAJECTORY** - For proof-of-principle, a simplest variable crank velocity profile, a sinusoidal wave form velocity at an average speed of 600rpm with a wave magnitude of +/-200rpm, has been employed in the study. Figure 5 shows the theoretical variable crank rotation velocity at varying crank position in comparison with an equivalent conventional constant speed one. The piston TDC position is 0 and 360 deg.

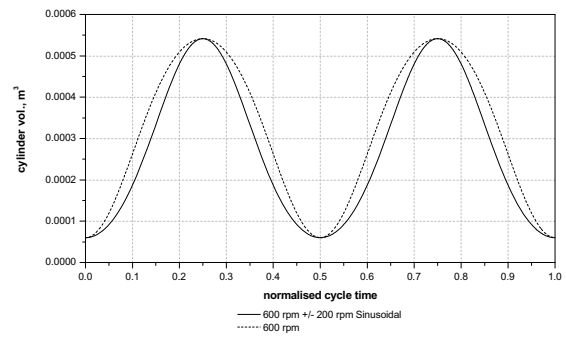


Figure 6: Cylinder volume at normalized cycle time with conventional and QCV cycles

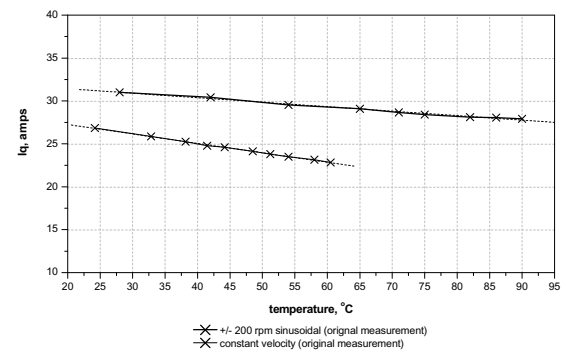


Figure 7: Motor current drift at varying operation temperature

The two crank rotation velocities drive the piston in very different profiles. Figure 6 shows the resulted cylinder volume at a normalized time scale over an entire 4-stroke engine cycle. 0 and 0.5 at the normalized scale represent the TDC position. It can be seen that the piston residual time at BDC is much longer than that at TDC with the conventional constant crank velocity, as shown by the dashed line. This is due to the kinematics of the crank-slider mechanism which gives an asymmetric piston velocity distribution between the journeys to TDC and to BDC from the middle of the stroke. As we know that the combustion happens at the TDC region. If a high efficiency thermodynamic cycle, Otto cycle for example, is to be used, a longer residual time at TDC rather than BDC is required. Clearly, the nature of the crank-slider mechanism prevents the potential combustion optimization by simply using the convention way of operating the IC engine in a constant crank rotation speed. In comparison, a sinusoidal crank rotation speed delivers a rather different piston movement profile. The residual time at TDC has been significantly extended, while the residual time at BDC is

reduced, as shown by the solid line. This offers longer time for the combustion event to complete at the TDC region which delivers higher combustion efficiency than the conventional one.

**ELECTRIC POWER** – In the  $d$ - $q$  model of the PMAC motor, the stator currents are transformed into an orthogonal frame of reference which is moving synchronously with the rotor flux. The orthogonal reference frame is derived from the phase currents via the nonlinear transform [11,12,13].

$$\begin{bmatrix} V_q \\ V_d \end{bmatrix} = \frac{2}{3} \begin{bmatrix} \cos(\theta) & \cos\left(\theta - \frac{2\pi}{3}\right) & \cos\left(\theta + \frac{2\pi}{3}\right) \\ \sin(\theta) & \sin\left(\theta - \frac{2\pi}{3}\right) & \sin\left(\theta + \frac{2\pi}{3}\right) \end{bmatrix} \begin{bmatrix} V_a \\ V_b \\ V_c \end{bmatrix} \quad (1)$$

where  $V_d, V_q$  are the d and q axis voltages,  $V_a, V_b, V_c$  are the three phase elements.

The system voltage drops in the synchronous frame are given as

$$V_q = ri_q + \omega Li_d + \omega \kappa + L \left( \frac{di_q}{dt} \right) \quad (2)$$

$$V_d = ri_d - \omega Li_q + L \left( \frac{di_d}{dt} \right) \quad (3)$$

where  $i_d, i_q$  are the d and q axis currents,  $r$  is the phase resistance,  $\omega$  is the rotor velocity,  $L$  is the phase inductance and  $\kappa$  is the back EMF constant in the reference frame as volts/radians/second.

The electrical torque developed by the motor is proportional to the q-axis current

$$T_e = k_t i_q \quad (4)$$

where  $k_t$  is the motor torque constant.

**THERMAL CALIBRATION** - The temperature significantly influences the electric conductivity of the materials used in the electric motor. Figure 7 shows the required current integral,  $I_q$ , over a 4-stroke engine cycle at varying motor temperature. The temperature influences on both scenarios, the conventional cycle and the QCV cycle using sinusoidal crank speed, were shown. It can be seen that as temperature increases,

the conductivity of the motor improves and the required electric current to drive the motor reduces. To use the motor current to evaluate the engine cycle performances, such temperature influences have to be corrected. Figure 8 shows the corrected current integral over the 4-stroke engine cycle for both conventional and the QCV cycles. The currents were calibrated to the value at 60°C. The current required to motor the engine in the conventional cycle is much less, 6 amps lower than that in the QCV cycle. This is simply due to the fact that the motor needs to deliberately accelerate and decelerate the crank in QCV cycle, while with the conventional cycle the motor is more or less to maintain a constant crank speed.

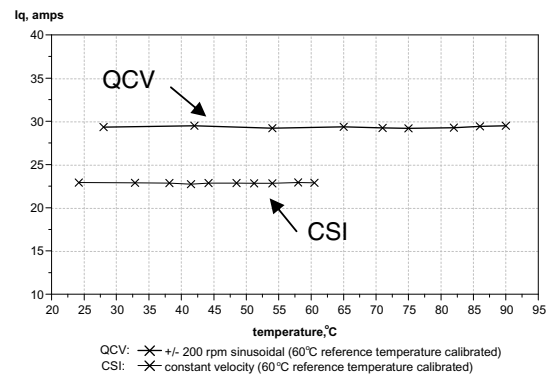


Figure 8: Corrected motor current at varying operation temperature

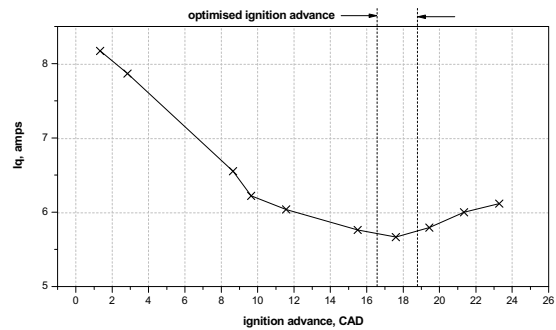


Figure 9 Spark ignition advance optimisation (constant speed)

**IGNITION OPTIMISATION** - Spark ignition timing is a critical parameter affecting the engine power output performances of both a conventional cycle and the QCV. It needs to be optimized to produce the maximum power. In this research work, the ignition timing optimization is



achieved by minimizing the required electric current to drive the single cylinder engine. Figure 9 shows a typical example with the conventional cycle. There is always a positive demand from the electric motor to complete the engine cycle. This is contributed by the fact that the single-cylinder engine employed by the project has no cooling system and it can only operate at very low load conditions for a limited period of time. At these low load conditions, the power produced by the combustion is insufficient to overcome the various losses. External power from the electric motor is needed to complete the cycle.

Still, the minimization of the required power shows the optimized region of the spark ignition timing. Figure 10 summarizes the optimized ignition timing for the two engine cycle scenarios. It is interesting to point out that the optimized ignition advances for the conventional cycle are significantly higher than the QCV cycle at all engine speeds tested. This is clearly due to the fact that the piston has a longer residual time at the TDC region with the QCV cycle, which can afford a later spark ignition timing but still has sufficient time for the combustion to complete in time before the piston moving away from the TDC region. Overall, the optimized spark ignition timing advances increases as the average engine speed increases. Again, this reflects the fact that the piston residual time at TDC region decreases as engine speed increases with both conventional and QCV cycles. The spark ignition timing has to be advances more to provide sufficient time for the combustion to complete. Even at the high speeds, the advances for the QCV cycle are lower than those for the conventional cycle.

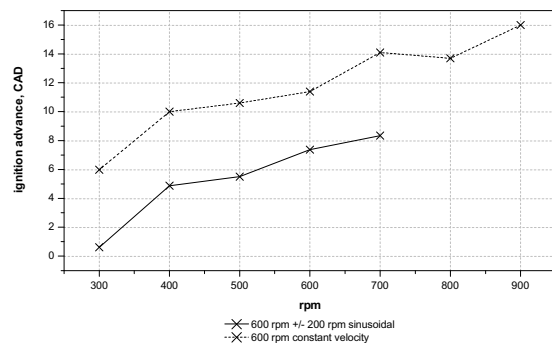


Figure 10: Optimised spark ignition advances at varying engine speed

## RESULTS AND DISCUSSION

**IN-CYLINDER PRESSURE** - Figure 11 and 12 show the motored cylinder pressure of a conventional cycle at 600rpm and a QCV cycle with a sinusoidal speed of 600rpm average with +/-200rpm amplitude at crank

angle and normalized time scale, respectively. The engine is 5.75% throttle opening in the conventional cycle and 5.3% for the QCV cycle. The slightly difference is to mock up the fired scenarios where for the same fuel injection pulse width of 5.65ms, these two different throttle openings are required to deliver the same stoichiometric combustion ( $\lambda = 1$ ). In other words, the engine volumetric efficiency has been improved about 8% by using the QCV cycle. This may due to the fact that the different piston trajectory as shown in Figure 6 results in different intake gas flow characteristics. With the QCV cycle, the piston movement is significantly slower than the conventional cycle during the intake stroke. This reduces the air flow velocity and therefore the throttling losses.

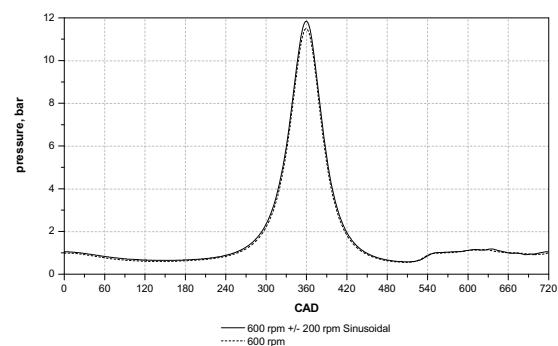


Figure 11: Motored cylinder pressure with conventional and QCV cycles vs. crank angle

Furthermore, it is interesting to note that the two different ways of presentation of the same set of measured in-cylinder pressure, via engine crank angle and normalized time scale, showed a rather different story. In the conventional way of presentation by using crank angle, the peak pressure of the QCV is about 3% higher than the conventional cycle. The same phenomenon exists in the plot against the normalized cycle time. However, the pressure traces during compression and expansion strokes are very different. With the crank angle, the pressure in both scenarios are about the same. However, with respect to the normalized time scale, the compression and expansion pressure of the QCV cycle is significantly higher that of the conventional one. Again, this is contributed to the fact that the piston with QCV cycle moves much slower at the high pressure region, the combustion TDC region, than that with the conventional cycle. In other words, the high pressure in the combustion TDC region will act on the piston for a longer time with the QCV cycle than that with the conventional one.

Figure 13 shows the fired cylinder pressure of the conventional cycle at 600rpm and the QCV cycle at a sinusoidal speed of 600rpm average with +/-200rpm

amplitude at a normalized cycle time. Again, the engine was 5.75% throttled in the conventional cycle and 5.3% for the QCV cycle. The fuel injection pulse width for both scenarios were same with 5.65ms. The spark ignition timing of the conventional cycle was optimized at 10.2°CA BTDC. For the QCV cycle, it was optimized at 9.8°CA BTDC. Clearly, the QCV cycle uses a later optimized ignition timing, but produces a later but higher peak cylinder pressure, which further leads to an overall higher in-cylinder pressure during the expansion stroke.

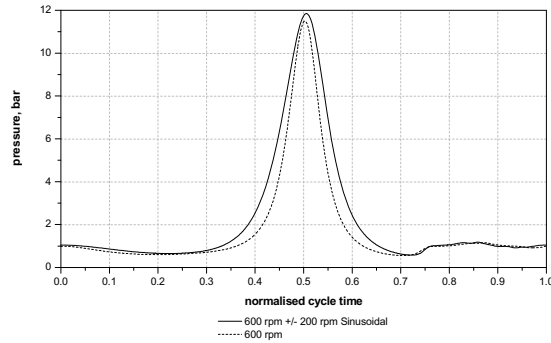


Figure 12: Motored cylinder pressure with conventional and QCV cycles at normalized cycle time

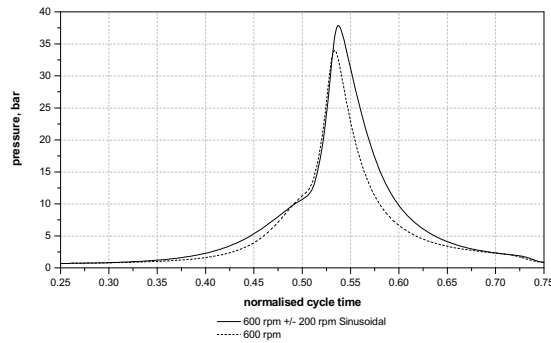


Figure 13: Fired cylinder pressure with conventional and QCV cycles

Table 1 Evaluation of cycle pressure integral at each engine stroke (bar)

Stroke	Motored		Fired		Change	
	CSI	QCV	CSI	QCV	CSI	QCV
Intake	0.729	0.816	0.739	0.780	0.010	-0.036
Compression	2.754	3.616	2.966	3.627	0.212	0.011
Combustion	2.544	3.269	8.834	10.799	6.290	7.530
Exhaust	1.022	1.035	0.876	0.850	-0.146	-0.185
<b>Cycle effective:</b>	<b>1.761</b>	<b>2.183</b>	<b>3.253</b>	<b>3.840</b>	<b>1.492</b>	<b>1.657</b>

The work produced by a combustion engine is an integration of the pressure over an engine cycle. Clearly, the higher expansion pressure of the QCV cycle can produce higher work than its conventional counterpart. To clarify the case, Table 1 summarizes the in-cylinder pressure integral of both conventional and QCV cycles via normalized cycle time. Pressure unit employed in the work is absolute pressure. All four strokes were then averaged by the normalized cycle time to show the cycle effective integral. Both motored and fired cycles were compared. The difference between the fired cycle and the motored one, the Change, is the net contribution by the combustion. The negative value in the different is showing that the pressure integral with the fired cycle is lower than the motored one. It happened with the QCV at intake and exhaust strokes and the CSI at exhaust stroke only. This is confirmed by that fact that the differences of the pressure integral among intake, compression and exhaust strokes between the fire and the motored cycles are minimal. Only the combustion stroke makes the contribution. Overall, the pressure integral of the QCV cycle is 11% higher than that of the conventional cycle.

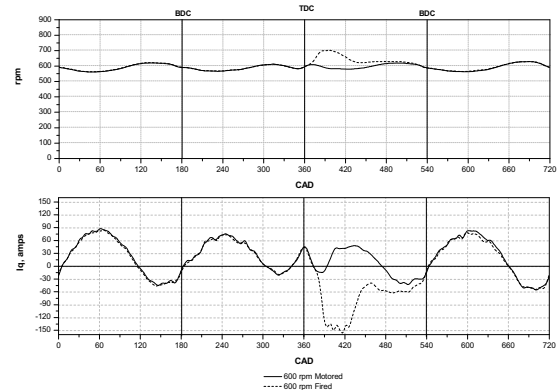


Figure 14: Motored and fired crank speed and motor current of conventional cycle

**ELECTRIC CURRENT** - Figure 14 shows the motored and fired engine crank speed (rpm) and the electric current ( $I_q$ ) of the conventional cycle at 600rpm. Although the engine is to be set at 600 rpm, the measured engine crank speed shows a small sinusoidal variation within each stroke with an amplitude of around  $\pm 30$  rpm. The fired cycle closely follows the motored cycle during intake, compression and exhaust strokes. There is a significant difference between the fired and the motored cycles within the combustion stroke. The fired cycle accelerate the engine significantly during the early part of the combustion stroke, then gradually reduces back to the level of the motored cycle towards the end of the stroke. This is due to the contribution of the combustion. Such contribution can be further

clarified by the measured electric current ( $I_q$ ) of the electric motor/generator. The positive value of the  $I_q$  stands for the current input into the electric motor/generator to drive the entire system, while the negative value shows the current generated from the system. The engine system employed in the research is a single cylinder research engine converted from a twin-cylinder engine base. It requires energy input to maintain the piston movement. This is shown by the fact that the positive current is significantly larger than the negative one among intake, compression and exhaust strokes. The combustion stroke of the fired cycle expands the measured current into large negative values. This is of course the power generated by the combustion.

Figure 15 shows the motored and fired engine crank speed (rpm) and the electric current ( $I_q$ ) of the QCV cycle with a sinusoidal speed of 600rpm average with  $\pm 200$ rpm amplitude. Clearly, the engine crank speed cannot follow the sinusoidal profile accurately. It starts the intake stroke at 400rpm at the TDC position, but overshoot before reaching the BDC at the designed speed of 800rpm. The control system has to reduce the overshoot crank speed before the TDC back to the designed level. The electric current input into the system to achieve such a variable speed is therefore much higher than the conventional constant speed one showed in Figure 14. Since the engine has a high speed, 800rpm, at the BDC position and it is designed to slow down the speed to 400rpm at the TDC, it requires significantly less power to compress the engine charge contributed to the piston decelerating kinetic energy. Similar story shared by the combustion and exhaust strokes. This, to a certain level, compromises the high power demands of the QCV cycle to accelerate and decelerate the engine to achieve the low engine speed at the TDC region. Table 2 summarizes the electric current integral of the motor/generator with both fired and motored cycles. As shown in the Figure 14 and 15, the current integral of QCV is over 3 times higher than that of conventional cycle during the intake stroke. However, this loss has been largely compensated by the following compression stroke where the QCV cycle is actually producing current. Overall, if the difference between fired cycle and the motored one is assumed to be the contribution from combustion, it can be seen that the QCV combustion produces about 15.8% higher electric current integral than that by the conventional one. This agrees, in principle, with the improvement found from the pressure integral.

However, it should be borne in mind that the piston trajectory followed was arbitrarily chosen to pass through TDC at low velocity - no attempt has yet been made to optimize the control algorithm. The motivation for the current proposal is to fully research the potential of this control regime, with particular reference to standard, commercially available, multi-cylinder IC engines. Further research will be to apply a great deal of

experience in multi-objective optimisation of aerospace and automotive systems to define the best combinations of solutions. In parallel with the optimal design procedure, the effect of the multi-physics system on emissions and fuel economy will be investigated.

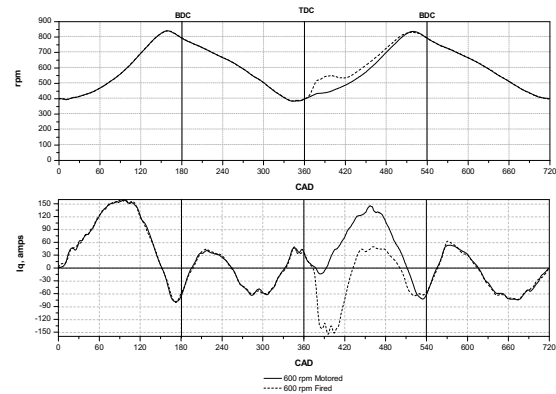


Figure 15: Motored and fired crank speed and motor current of QCV cycle

Table 2 Evaluation of cycle corrected current at each engine stroke (Amps)

Stroke	Motored		Fired		Change	
	CSI	QCV	CSI	QCV	CSI	QCV
Intake	21.48	75.90	20.48	76.25	-1.00	0.35
Compression	27.36	-6.35	27.94	-7.51	0.58	-1.16
Combustion	2.83	49.94	-67.91	-31.24	-70.74	-81.18
Exhaust	19.65	-22.79	18.25	-23.47	-1.40	-0.68
<b>Cycle effective:</b>	<b>17.90</b>	<b>24.10</b>	<b>0.99</b>	<b>4.52</b>	<b>-16.91</b>	<b>-19.58</b>

Reducing the piston speed at the TDC position reduce the kinematic losses, but will ignite further variations in heat transfer and mass blowby, which may further affect the emissions and piston reliability. These will addressed in future further studies.

The QCV concept discussed in the paper is based on a single cylinder case. The concept has a potential for multi-cylinder applications where the phase angle between neighboring cylinders will have to be the cycle time of the crankshaft angular speed variation. For example, if the engine has a phase angle of  $180^\circ$ , such as two or four cylinders in-line design, the crankshaft deceleration will have to be at both TDC and BDC positions. This will be investigated in future further studies.

The proof-of-principle experimental study was done at 600 rpm. The concept is suitable higher speeds. However, the engine used in the project has an over-

weighted piston assembly by adding the stiff steel bar for the extension which causes excessive loading to the crank. The hardware design has to be optimized for high speed studies.

## CONCLUSION

The QCV concept proposed in this study can be hybridized with a sophisticated combined electric motor and generator unit to form a series-hybrid power-train to deliver the much desired high fuel efficiency and low pollutant emissions powertrain system with good power output.

A proof-of-principle system has been developed. It consists of a high torque-to-inertia, high bandwidth, permanent magnet brushless AC electric machine, a single-cylinder research Spark Ignition (SI) engine, and a control system.

Two engine crank speed profile have been employed in the study, a constant 600rpm for a conventional cycle and a QCV cycle with a sinusoidal speed of 600rpm average with +/-200rpm amplitude. It found that with the conventional constant crank speed, the piston residual time at BDC is much longer than that at TDC. However, the chosen QCV cycle changes the piston movement profile and produces longer residual time at TDC to favour the combustion optimisation.

With the QCV cycle, the piston movement is significantly slower than the conventional cycle during the intake stroke. This reduces the air flow velocity and therefore the throttling losses. The engine volumetric efficiency has been improved about 8% by using the QCV cycle.

The work produced by a combustion engine is an integration of the pressure over an engine cycle. Clearly, the higher expansion pressure of the QCV cycle can produce higher work than its conventional counterpart. Overall, the pressure integral of the QCV cycle is 11% higher than that of the conventional cycle.

The measure electric motor/generator current integral is another indicator of the system power output or requirement. The experimental results showed that the QCV combustion produces about 15.8% higher electric current integral than that by the conventional one.

## ACKNOWLEDGMENTS

The authors would to thank the Engineering, Physics and Science Research Council (EPSRC), UK for funding the preliminary research which forms the foundation of this project and the Lotus Engineering for the facility support.

## REFERENCES

1. Stone R., 'Introduction to Internal Combustion Engines (3rd Edition)', Macmillan Press Ltd London, ISBN 0-333-74013-0, 1999.
2. Ge Y., Chen L., Sun F., Wu C., 'Thermodynamic simulation of performance of an Otto cycle with heat transfer and variable specific heats of working fluid', International Journal of Thermal Sciences, vol. 44(5), 2005, pp.506-511
3. Shi L., Cui Y., Deng K., Peng H., Chen Y., 'Study of low emission homogeneous charge compression ignition (HCCI) engine using combined internal and external exhaust gas recirculation (EGR)', Energy, vol. 31(14), 2006, pp.2665-2676
4. Maggetto G., Van Mierlo J., 'Electric vehicles, hybrid electric vehicles and fuel cell electric vehicles : state of the art and perspectives', Annales de Chimie Science des Matériaux, vol. 26(4), 2001, pp.9-26
5. Zhong L., Rahman M.F., Hu W.Y., Lim K.W., 'Analysis of direct torque control in permanent magnet synchronous motor drives' IEEE Trans on Power Electronics, vol. 12, no. 3, 1997, pp.528-536.
6. ABB, 'Direct torque control – the world's most advanced AC drive technology', Technical Guide.
7. Liu Y., Zhu Z.Q., Howe D., 'Direct torque control of brushless DC drives with reduced torque ripple', IEEE Trans. on Industry Applications, vol. 41, no. 2, 2005, pp.599-608.
8. Zhu Z.Q., Liu Y., Howe D., 'Comparison of performance of brushless DC drives under direct torque control and PWM current control', Korean IEE Int. Trans. On Electrical Machinery and Energy Conversion Systems, vol. 5-B, no. 4, 2005, pp.337-342.
9. Stewart P., Stone D.A., Fleming P.J. "Design of robust fuzzy-logic control systems by multi-objective evolutionary methods with hardware in the loop" IFAC Journal of Engineering Applications of Artificial Intelligence, Vol.70, no.3, 2004, pp.275-284.
10. Zhu Z.Q. and Howe D., 'Halbach permanent magnet machines and applications: a review', IEE Proc. Electrical Power Applications, vol. 148, no. 4, pp.299-308, 2001.
11. Pillay P., Krishnan R., "Modelling, simulation, and analysis of permanent magnet motor drives, Part 1: The permanent magnet synchronous motor drive", IEEE Transactions on industrial applications, vol.25, no.2, pp265-273, March/April 1989.
12. Hindmarsh J., "Electrical machines and drives", Pergamon Press Ltd. UK, 1985, ISBN 0-08-031684-0.
13. Kim J.M., Sul S.K., "Speed control of interior permanent magnet synchronous motor drive for the flux-weakening operation", IEEE Transactions on Industrial Applications, vol.33, no.1, pp43-48, Jan/Feb 1997.